Excitation wavelength dependent fluorescence anisotropy of eosin-myosin adducts

Evidence for anisotropic rotations

D.L. VanderMeulen [a], D.G. Nealon [a,c], E. Gratton [b] and D.M. Jameson [c,d]

[a] *Baylor Research Foundation, Dallas, TX 75246,* [b] *Laboratory for Fluorescence Dynamics, Department of Physics, University of Illinois, Urbana, IL 61801,* [c] *Pharmacology Department, University of Texas Southwestern Medical Center, Dallas, TX 75235 and* [d] *Department of Biochemistry and Biophysics, University of Hawaii, Honolulu, HI 96822, U.S.A.*

Steady-state and time-resolved fluorescence anisotropy measurements of eosin in solution and eosin-5-maleimide bound to purified myosin were made to study localized motions of the "head region" of this protein. The lifetime and apparent Debye rotational relaxation times of eosin in aqueous solution are essentially invariant with changes in excitation wavelength. In more viscous solvents, such as propylene glycol/water mixtures, the apparent Debye rotational relaxation times of eosin differ upon excitation in the regions of positive and negative anisotropy. Using eosin attached to the SH-1 thiol of the myosin head differing rotational modes of the bound probe were detected, dependent upon excitation wavelength. The main features of the anisotropy data for eosin-myosin are consistent with the existence of a 'crevice' or 'pocket' in the myosin head. A model is presented which allows estimation of the ratio of distinct rotational diffusion terms (selected by different excitation wavelengths) that produce both the observed steady-state anisotropy and differential phase results.

1. Introduction

Time-resolved and steady-state fluorescence anisotropy studies have been increasingly utilized to investigate dynamics of complex proteins and other macromolecules (ref. 1, and references cited therein). In particular, there have appeared both theoretical and experimental studies of dyes, dye-protein adducts, intrinsic protein chromophores, and membrane systems capitalizing to some degree on the excitation wavelength dependence of certain spectroscopic probes [2–13]. In an effort to enhance the interpretation of our preliminary

studies [11–13], we investigated in further detail certain analytical aspects of the relationship between wavelength-dependent fluorescence anisotropy data and rotational motions. In this report we utilize the well-studied protein myosin in conjunction with the luminescence probe eosin.

Recent evidence has reinforced the fundamental importance of the 'head' region of myosin in contractile function [14]. It appears that the flexibility and relative dynamic motional properties of the major structural 'subdomains' are important in the contractile process. Time-resolved biophysical studies have demonstrated that myosin heads are segmentally flexible about a swivel-like connection to the filamentous tail (refs 15 and 16, and references cited therein). More localized 'internal' motions of the head region and their relationship

Correspondence address: D.L. VanderMeulen, CINN Research, Columbus Medical Center, 2520 N. Lakeview Ave, Chicago, IL 60614, U.S.A.

to the enzymatic or contractile function have yet to be fully characterized. The experimental support derives from ^{1}H-NMR and transient electrical birefringence data (17,18).

As data from oxygen quenching and related spectroscopic experiments have shown, local, rapid internal motions of a protein structure are common. Proteins or other biopolymers thus cannot generally be represented solely in terms of a rigid hydrodynamic ellipsoid or similar model [19]. Depending on the time scale monitored, the motions of a fluorophore, its environment and the protein as a whole need to be incorporated into what has been termed a 'restricted flexible model' [20].

We have thus made fluorescence anisotropy measurements of myosin labeled with specific site-directed probes capable of monitoring both fast, 'localized' motions, as well as relatively slower, more 'global' rotations. Steady-state and time-resolved measurements were performed at different excitation wavelengths in order to increase the information content on the probe's rotational modes. This approach involves the photoselection of transition dipole moments exhibiting significantly different orientations [2,5,10–13]. Excitation wavelength dependent steady-state Perrin-Weber anisotropy data were originally interpreted [12] according to a model considering rotational correlation times, corresponding to anticipated motional rates for the protein, a protein subdomain and the probe itself. The data were fitted using a nonlinear least-squares approach [21]; in that work, however, it was generally necessary to incorporate opposing or 'negative' relative motions to produce a satisfactory fit. Further consideration of the relationship between experimental results and all their potential theoretical bases has now led to an apparently more fundamental explanation. Presented here are experimental data, as well as a discussion of specific aspects of analysis germane to their interpretation.

2. Materials and methods

Eosin Y lactone was purchased from Aldrich and eosin-5-maleimide was obtained from Molecular Probes; dye purity was monitored by silica

gel thin-layer chromatography. Sucrose for the isothermal fluorescence anisotropy measurements was obtained from Sigma or Aldrich and recrystallized two to three times from methyl alcohol to minimize the presence of impurities as monitored by fluorescence spectra obtained with ultraviolet (e.g., 350 nm) excitation. Buffers and other chemicals were highest quality analytical reagent grade.

Myosin and the chymotryptic S-1 subfragment (lacking the filamentous tail) were prepared from rabbit skeletal muscle as described with minor modifications [22–25]. Since small amounts of other muscle proteins may be present in this preparation, and since fluorescence anisotropy results may be sensitive to the presence of any nonspecifically labeled low molecular weight impurities, we further purified myosin using DEAE-cellulose ion-exchange chromatography or using an agarose-hexane-ADP affinity gel (P & L Biochemicals). Preparation purity was checked by SDS gel electrophoresis with Coomassie blue staining of protein bands. Myosin ATPase activity was monitored by the pH stat method [26]; with 0.1 mg in 2 ml reaction mixture at 25°C (1 mM Tris-maleate, 10 mM $CaCl_2$, 2 mM ATP, pH 8), activity was typically 1 μmol/min per mg.

Eosin was conjugated to the SH-1 thiol of the (20 kDa domain) of myosin following the procedure of Kinosita et al. [27]. Unreacted dye was removed with a 10 cm Sephadex G-25 desalting column (Pharmacia) and/or extensive dialysis against buffer at 5°C. Buffer for solubilizing myosin was 500 mM KCl, 10 mM Mops, 0.1 mM EDTA, pH 7. Protein concentrations were primarily measured using ultraviolet absorption methods [23]. For fluorescence measurements, the absorbance of the preparation at the wavelength of excitation was adjusted to below 0.1 to avoid artifacts.

Excitation polarization spectra were recorded on a T-format fluorescence spectrometer (either an SLM-Aminco 8000 or a laboratory-built instrument of comparable design). For display clarity, data for these excitation spectra are presented in terms of polarization (p), while all other figures utilize anisotropy (r); these are directly related by the expression: $r = 2p/(3 - p)$. Isothermal Perrin-Weber plots at 5°C were made by varying

the solution viscosity with sucrose additions; where necessary, background counts of the medium (minus fluorophore label) were subtracted. The value of r_0/r is plotted vs T/η, where r_0 is the anisotropy of the dye immobilized in glycerol at $-20\,°C$, T the absolute temperature (in K) in the sample cuvette monitored by a thermistor, and η the solution viscosity (in cP).

Time-resolved fluorescence measurements were carried out using a multifrequency phase fluorometer based on the instrumentation of Gratton and Limkeman [28]. In the multifrequency phase and modulation approach to time-resolved measurements, the intensity of the exciting light is modulated and the phase shift and relative modulation of the emitted light, with respect to the excitation, are determined [29].

In addition to fluorescence lifetime determinations, the multifrequency phase and modulation method permits characterization of the rotational modes of a fluorescence molecule [30,31]. In the time domain, such information is obtained from anisotropy decay data; the frequency domain equivalent of these data is obtained by differential polarized phase fluorometry (also known as dynamic polarization). In this approach, the sample is illuminated by parallel polarized light, the intensity of which is modulated at high frequencies. The phase delay between the parallel and perpendicular components of the emission ($\phi_{\parallel}$ and $\phi_{\perp}$) are determined and the differential phase function ($\Delta\phi$) may be calculated as [29]:

$$\Delta\phi = \phi_{\parallel} - \phi_{\perp}$$

where, for an isotropic rotating molecule,

$$\Delta\phi = \{18\omega r_0 R\}/\{[(k^2 + \omega^2)(1 + r_0 - 2r_0^2)] + 6R(6R + 2k + kr_0)\}$$

where r_0 is the limiting anisotropy, R the rotational diffusion coefficient, k the radiative decay rate constant $(1/\tau)$ and ω the angular modulation frequency.

The corresponding expression for the differential modulation ratio is

$$\left(\frac{M_{\parallel}}{M_{\perp}}\right)^2 = \frac{[(1 - r_0)k + 6R]^2 + (1 - r_0)^2\omega^2}{[(1 + 2r_0)k + 6R]^2 + (1 + 2r_0)^2\omega^2}$$

where $M_{\parallel}$ and $M_{\perp}$ are the respective demodulation ratios for the parallel and perpendicular emitted components.

Analysis of the phase decay (or modulation ratio) vs frequency curves thus permits one to characterize the fluorophore's rotational parameters. The data can be fitted to a range of models including anisotropic rotators and combinations of global and local rotations which have been demonstrated in a number of fluorophore-protein cases.

Computer analysis and fitting of steady-state and time-resolved anisotropy data were accomplished using software from ISS (Champaign, IL). The essential equations are given below:

$$I_{\parallel}(t) = g(1 + 2r_{(-)}(t))e^{-t/\tau} + (1 - g)(1 + 2r_{(+)}(t))e^{-t/\tau}$$

$$I_{\perp}(t) = g(1 - r_{(-)}(t))e^{-t/\tau} + (1 - g)(1 - r_{(+)}(t))e^{-t/\tau}$$

where $r_{(-)}(t)$ and $r_{(+)}(t)$ correspond to the decay of the anisotropies excited at the negative and positive regions of the excitation polarization spectrum, respectively, and g is the relative fraction of the observed decay due to each individual decay. The steady-state anisotropy, r_{ss}, is then given by:

$$r_{ss} = \frac{\langle I_{\parallel}\rangle - \langle I_{\perp}\rangle}{\langle I_{\parallel}\rangle + 2\langle I_{\perp}\rangle}$$

where the $\langle I_{\parallel}\rangle$ and $\langle I_{\perp}\rangle$ indicate time-averaged values. The standard deviation of each individual data point was assumed to be 0.2 and 0.004° for the phase and modulation, respectively. This assumption can produce a χ^2 value different from 1, if the red standard deviations are different. However, the values of the parameters are unaffected by the common value of the weight.

3. Results

Excitation polarization spectra recorded under conditions where the rotational and translational motions of the dye are fully restricted demonstrate
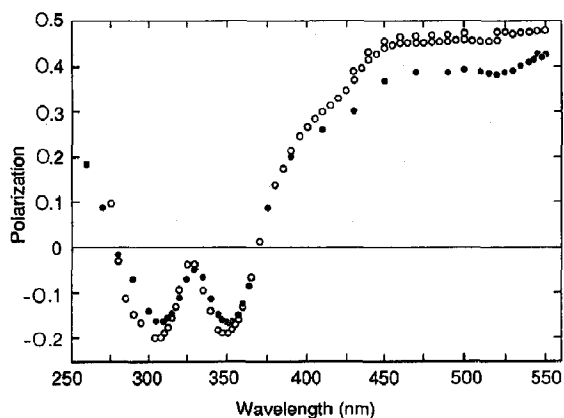
Fig. 1. Excitation polarization spectra of eosin-5-maleimide adducts of N-acetylcysteine in glycerol (open symbols) and myosin in buffer (closed symbols). Both samples were thermostatted at 5°C. Excitation bandwidth was 2 nm and emission was monitored through a cutoff filter (Schott GG089) which passed wavelengths longer than 550 nm.

wavelength dependence of the intrinsic or limiting polarization, p_0 (or anisotropy, r_0). The excitation polarization spectra of eosin-5-maleimide covalently linked to myosin and to the model compound N-acetylcysteine are shown in fig. 1. Excitation into the lowest energy absorption band (e.g., > 500 nm) yields high, positive p_0 values, whereas absorption by higher energy bands with a different orientation of the absorption dipole (e.g, at 310 and 350 nm) produces negative values. The major features of wavelength dependence of dipole orientation for eosin are retained upon binding to the protein. The absorption dipoles for transition moments excited by 350 and 514 nm radiation are nearly normal one to another, whereas the emitted fluorescence arises from the same dipole for either excitation wavelength.

The steady-state polarization of eosin-myosin excited at 514 nm was 0.40 ± 0.01 in buffer at 5°C. On the other hand, the p_0 for eosin is approx. 0.47. If measurements are made in a buffer solution containing 70% glycerol at -2°C, the polarization of free eosin is still relatively high (0.445 ± 0.005), whereas p_0 for eosin-myosin remains comparatively low (0.40).

Rotational information from steady-state measurements was obtained using Perrin-Weber anisotropy plots recorded by varying the solvent

viscosity at a constant temperature. Isothermal plots have the advantage of eliminating the temperature-dependent activation of thermal rotational modes of the system. The data points in fig. 2A and B show the values of the fluorescence anisotropy of the eosin-myosin and eosin-cysteine conjugates, respectively, with excitation wavelengths of 350 and 514 nm at various viscosities. Results are presented in a standard format normalized to the value of r_0. The linear response of the plot in fig. 2B shows that eosin free in solution exhibits isotropic hydrodynamic behavior, since no significant differences in rotational behavior are observed, even when absorption dipoles of markedly differing orientation are excited. On the other hand, restricted motion and anisotropic rotations are exhibited by the protein-bound probe
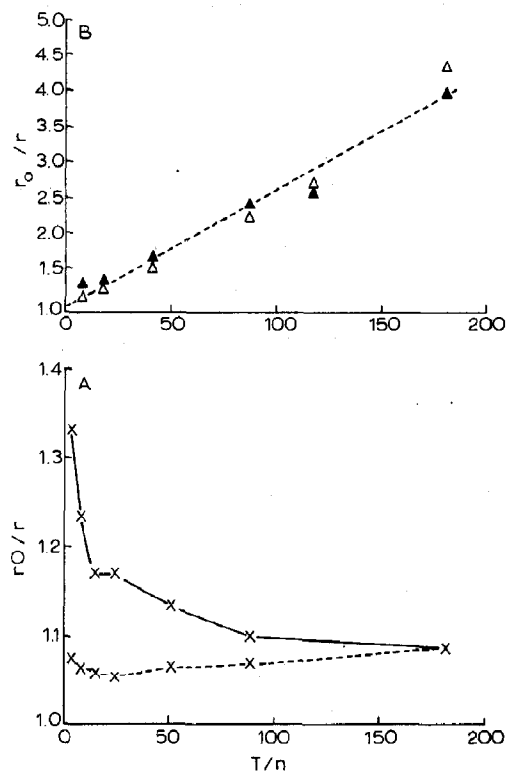

Fig. 2. (A) Isothermal Perrin-Weber anisotropy plot of eosin-5-maleimide adduct of myosin in buffer with excitation at 514 nm (lower curve) and 350 nm (upper curve). (B) Isothermal Perrin-Weber anisotropy plot of eosin Y in buffer with excitation at 514 nm (open symbols) and 350 nm (closed symbols).
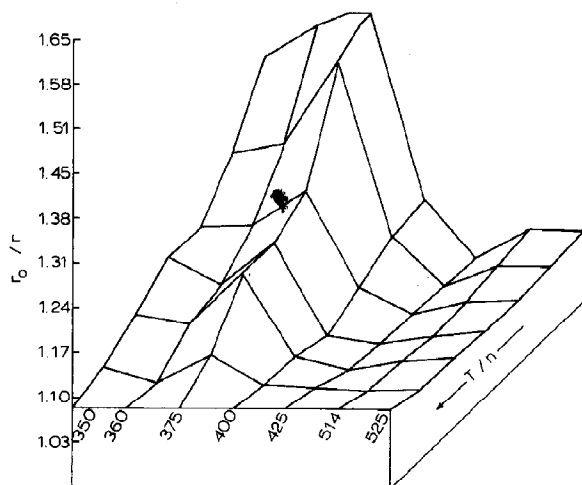
Fig. 3. Three-dimensional contour plot of isothermal Perrin-Weber anisotropy data for eosin-5-maleimide adduct of myosin in buffer at 5°C with seven different excitation wavelengths. Maximum value of r_0/r at 360 nm was 1.4. Emission monitored through cutoff filters (Schott GG087 + KV399). Maximum absorbance was less than or equal to 0.06.
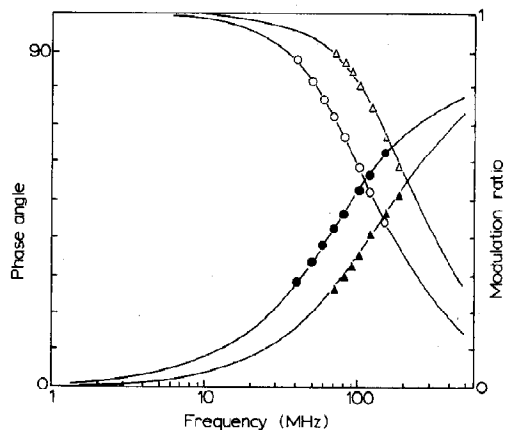

Fig. 4. Phase (closed symbols) in degrees and modulation (open symbols) lifetime data for eosin Y (triangles) and eosin-5-maleimide-myosin adduct (circles) recorded at 20°C. The solid lines indicate the best nonlinear least-squares fit as listed in table 1. Data for excitation at 351 and 514 nm were indistinguishable.

(fig. 2A). A more detailed examination of excitation wavelength dependent Perrin-Weber plots is shown in fig. 3.

Data for measurements of fluorescence lifetimes of eosin by multifrequency phase and modulation fluorometry are presented in fig. 4. The lifetimes are essentially invariant with changes in excitation wavelength (351 and 514 nm) for both free and protein-bound dye. We did observe a typical lengthening of the lifetime upon binding (~ 1.2 ns for eosin Y and 2.2 ns for eosin-myosin). These data show that differences in rotational behavior based on wavelength-dependent fluorescence anisotropy results are not due simply to different excited-state lifetimes.

As for steady-state anisotropy data presented above, differential phase (dynamic polarization) measurements show clear wavelength-dependent differences in the apparent rotational modes of bound probe (fig. 5). For 351 or 514 nm excitation of free eosin, rotation is essentially isotropic, with a Debye rotational relaxation time of approx. 0.4 ns. Bound to myosin, however, two components are evident for 351 and 514 nm, as summarized in table 1. The fractional weighting of the faster rate

was considerably smaller for 351 nm (< 0.1) than for 514 nm (> 0.4), thus providing evidence for highly anisotropic rotation. Experimental data for eosin linked to the S-1 myosin head subfragment did not show any significant difference from that of eosin-myosin (not shown).

For comparison, dynamic polarization data for eosin Y in 90% propylene glycol are shown in fig. 6 and table 1. Although the steady-state polarization for eosin in this system is comparable to that
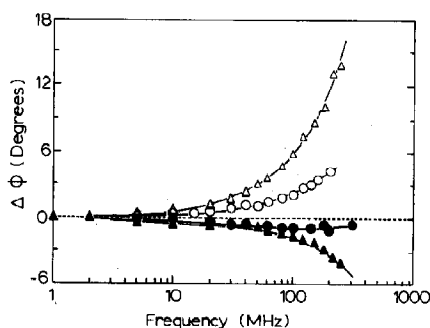

Fig. 5. Differential phase data for eosin Y (excitation: △, 514 nm; ▲, 351 nm) and eosin-5-maleimide-myosin adduct (excitation: ○, 514 nm; ● 351 nm) excitation at 20°C. The best nonlinear least-squares fit for component Debye rotational relaxation times and fractional contributions is reported in table 1.

Table 1

Summary of lifetimes (τ, in ns) and Debye rotational relaxation times (D, in ns) for eosin Y and EMI-myosin

| | Excitation wavelength (nm) | | | | | |
| | 514 | | | 351 | | |
	τ_1	f_1 [a]	χ^2	τ_1	f_1 [a]	χ^2
Intensity decay						
Eosin Y						
Buffer [b]	1.16	0.99	3.91	1.18	1.00	2.77
Propylene glycol/H_2O	2.47	1.00	2.65	2.41	1.00	6.94
EMI-myosin						
Buffer [b]	2.16	0.99	1.13	2.25	1.00	2.19

| Anisotropy decay | | | | | | | | |
	ρ_1	a_1	ρ_2	a_2	ρ_1	a_1	ρ_2	a_2
Eosin Y								
Buffer [b]	0.57	0.36	–	–	0.45	−0.125	–	–
Propylene glycol/H_2O	15.6	0.36	–	–	10	−0.125	–	–
EMI-myosin								
Buffer [b]	390	0.21	0.42	0.15	150	−0.115	2.50	−0.010

[a] In some cases a small component attributed to scattering was used with τ_2 fixed at 0.001 ns in order to improve the fit.
[b] Buffer consisted of 0.5 M KCl, 10 mM Mops (pH 7.0), 0.2 mM EDTA.

measured for eosin-myosin, the rotational behavior is essentially isotropic. The Debye rotation relaxation time for both excitation wavelengths is reduced by a little more than an order of magnitude, from approx. 0.5 to 10–15 ns, as expected for the more viscous environment.

4. Discussion

Nonconventional Perrin-Weber plots, such as fig. 2A, can simply arise from the superposition of two anisotropy terms, one with positive and the other with negative limiting anisotropy. Furthermore, the two anisotropy terms must respond to rotations of the system in a different way. For this effect to occur, the particular alignment of the emission dipole, which is selected by the different excitation wavelength, must also preferentially select two very distinct rotational diffusion terms. In our experiments, this occurrence is reflected in several spectroscopic properties including the steady-state excitation polarization spectrum which is dependent on the excitation wavelength but has a different shape at different values of T/η (see fig. 3).

To obtain a qualitative estimation of the ratio of diffusion coefficients for the two principal axes, selected by the different excitation wavelengths,
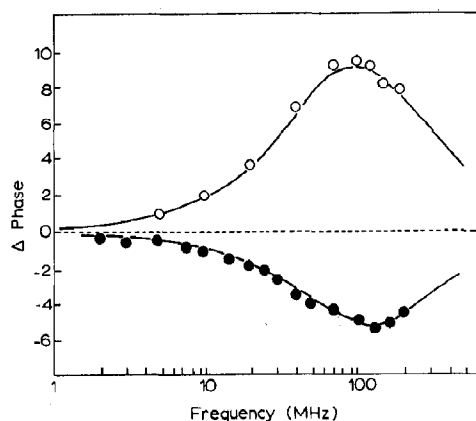

Fig. 6. Differential phase data (in degrees) for eosin Y in 90% propylene glycol/10% water with excitation at 514 nm (open symbols) and 351 nm (closed symbols). The solid lines indicate the best nonlinear least-squares fit for component Debye rotational relaxation times and fractional contributions, as listed in table 1.
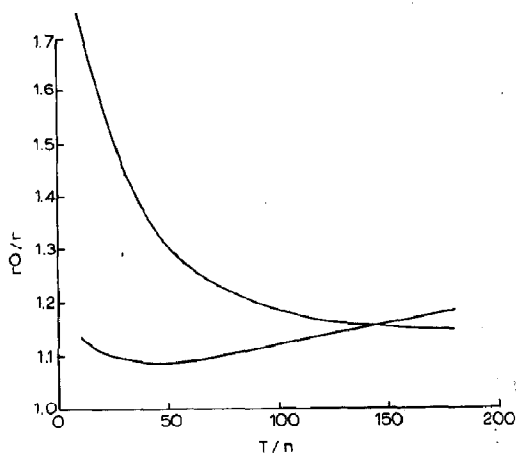
Fig. 7. Simulation of Perrin plots using the addition of two rotational species using the following parameters: $\tau = 2.1$ ns, $r_{01} = 0.36$, $r_{02} = -0.125$. The rotational relaxation time used for the simulations roughly corresponds to the value reported in table 1. It was assumed that viscosity affects the rotational relaxation times in a manner according to the Stokes-Einstein relationship. The two curves correspond to a value of $g = 0.915$ and 0.253 for the lower and upper curve, respectively.

we consider a simplified model in which the orientations of the two transition dipole moments coincide with the principal axes. This assumption will lead to an evaluation of the minimum asymmetry which is compatible with the experimental results. Since we observe a quantity which is proportional to an 'average projection' of the transition dipole moments on the principal axis, our model can only evaluate that projection. The effective asymmetry can, of course, be larger. For each of the two motions, we assume free rotation. We are well aware that the rotational motion is more likely restricted, but again, we are interested in the order of magnitude of the asymmetry ratio.

Simulations based upon this model are shown in fig. 7 for the steady-state Perrin-Weber plots. These stimulations illustrate the effect of increasing the fractional contribution of the negative polarization component. The simulations qualitatively reproduce the observed behavior of the steady-state polarization and differential phase measurements.

Comparison of the data for free eosin with the eosin-myosin data suggest that when bound, the probe exhibits anisotropic rotational motion. Excitation at both 351 and 514 nm reveals a very slow rotational component (> 100 ns), presumably due to the global motion of the large (480 kDa) protein. In addition, excitation into the 514 nm dipole direction results in a relatively fast subnanosecond component, similar in rate to freely rotating eosin in aqueous solution (table 1). On the other hand, excitation into the 351 nm dipole (approximately at 90° relative to the 514 nm transition moment) reveals a somewhat slower rotational component of a few nanoseconds for both steady-state and dynamic polarization. For perspective, the latter can be compared to the approx. 10 ns rotational relaxation time for free eosin in 'viscous' propylene glycol water solution (fig. 6).

Considering the steady-state polarization values for free eosin and eosin-myosin in 70% glycerol (cf. section 3), if the bound eosin were substantially exposed to the glycerol solution, one might expect a value closer to that for free dye in the same viscous environment. One can speculate concerning the potential shielding effect of a protein 'pocket'. The analysis of the differential phase data (table 1) indicates there is indeed a rapid rotation of the fluorophore consistent with the steady-state results. Corroborative measurements have been reported based on fluorescence energy transfer of several probes bound to myosin [32]. Those data pointed to a rather large 'hydrophobic crevice' on each head, large enough to accommodate several aromatic rings, including MgATP and a probe bound to the SH-1 thiol. Though conjectural, this structural arrangement may facilitate the enzymatic functioning of myosin.

Acknowledgements

References

1 D.M. Jameson and G.D. Reinhart, Fluorescent biomolecules: Methodologies and applications (Plenum, New York, 1989).

2 R. Memming, Z. Phys. Chem., Neue Folge 28 (1961) 168.

3 B. Withold and L. Brand, Biochemistry 9 (1970) 1948.

4 J.B. Ross, K.W. Rousslang and L. Brand, Biochemistry 20 (1981) 4361.

5 M.D. Barkley, A.A. Kowalczyk and L. Brand, J. Chem. Phys. 75 (1981) 3581.

6 M. Vincet, B. de Foresta, J. Gallay and A. Alfsen, Biochemistry 21 (1982) 708.

7 P.L.G. Chong, B.W. van der Meer and T.E. Thompson, Biochim. Biophys. Acta 813 (1985) 253.

8 S. Kinoshita, T. Fukami, Y. Ido and T. Kushida, Cytometry 8 (1987) 35.

9 K. Ajtai and T.P. Burghardt, Biochemistry 26 (1987) 4517.

10 W.A. Wegener, Biophys. J. 46 (1984) 795.

11 D.L. VanderMeulen and W.A. Wegener, Biophys. J. 47 (1985) 467.

12 D.L. VanderMeulen, B.W. van der Meer, V. Thomas and D.M. Jameson, Biophys. J. 49 (1986) 334.

13 D.G. Nealon, D.L. VanderMeulen and D.M. Jameson, Biophys. J. 53 (1988) 87.

14 T.R. Hynes, S.M. Block, B.T. White and J.A. Spudich, Cell 48 (1987) 953.

15 D.D. Thomas, J.C. Seidel, J.S. Hyde and J. Gergely, Proc. Nat. Acad. Sci. U.S.A. 72 (1975) 1724.

16 M.F. Morales, J. Borejdo, J. Botts, R. Cooke, R.A. Mendelson and R. Takashi, Annu. Rev. Phys. Chem. 33 (1982) 319.

17 S. Highsmith, K. Akasaka, M. Konrad, R. Goody, K. Holmes, N. Wade-Jardetzsky and O. Jardetzsky Biochemistry 18 (1979) 4238.

18 S. Highsmith and D. Eden Biochemistry 25 (1986) 2237.

19 G. Weber, in: Excited states of biological molecules, ed. J.B. Birks (Wiley, London, 1986) p. 363.

20 P. Wahl and G. Weber, J. Mol. Biol. 30 (1967) 371.

21 A.U. Acuna and M.P. Lillo, in: Fluorescent biomolecules: Methodologies and applications, eds. D.M. Jameson and G.D. Rinehart (Plenum, New York, 1986) p. 353.

22 Y. Tonomura, P. Appel and M. Morales, Biochemistry 5 (1966) 515.

23 S. Lowey, Methods Enzymol. 85B (1982) 55–71.

24 E.G. Richards, C.-S. Chung, D.B. Menzel and H.S. Olcott, Biochemistry 6 (1967) 528.

25 H.R. Trayer and I.P. Trayer, FEBS Lett. 54 (1975) 291.

26 H. White, Methods Enzymol. 85B (1982) 698.

27 K. Kinosita, Jr., S. Ishiwata, H. Yoshimura, H. Asai and A. Ikegami, Biochemistry 24 (1984) 5963.

28 E. Gratton and M. Limkeman, Biophys. J. 44 (1983) 315.

29 E. Gratton, D.M. Jameson and R.D. Hall, Annu. Rev. Biophys. Bioeng. 13 (1984) 105.

30 G. Weber, J. Chem. Phys. 66 (1977) 4081.

31 W.W. Mantulin and G. Weber, J. Chem. Phys. 66 (1977) 4092.

32 R.P. Haugland, J. Supramol. Struct. 3 (1975) 338.